Combustion Chamber Acoustics and its Interaction with LOX/H_2- and LOX/CH_4-Spray Flames

By Michael OSCHWALD, Bernhard KNAPP, Mark SLIPHORST, Mark MARPERT

German Aerospace Center (DLR), Institute of Space Propulsion, Lampoldshausen, Germany

The acoustics of combustion chambers and the interaction of acoustics and combustion is investigated in a model combustor operated with LOX/H_2 and LOX/CH_4. Acoustic excitations are induced by a siren during hot fire tests and the response of atomization and combustion is recorded with dynamic pressure sensors and high speed OH-imaging is applied. By analyzing the temporal and spatial distribution of the flame response the question is addressed, whether in the experiments the coupling of acoustics to combustion is via pressure or velocity sensitive processes. In the experiments it appeared that the acoustic eigenmodes of the combustor are characteristically deviating from cylinder modes. The results obtained can be explained by a modal analyses of the combustor geometry. These investigations have been extended to study the influence of absorbers and absorber rings on the acoustics of combustion chambers and resonance frequencies predicted by modal analysis and experimental results are presented.

Key Words: liquid propulsion, spray combustion, combustion instability

Nomenclature

I	: intensity of chemiluminescence
L	: length
N	: response factor
p	: pressure
$\dot{q}$	: heat release rate
u	: velocity
We	: We-number. $We = \rho d (u_{fuel} - u_{lox})^2 / \sigma$
x, y	: spatial coordinates
Δ	: peak-to-peak value
σ	: surface tension
Subscripts	
c	: combustor
a	: absorber

1. Introduction

The interaction of a resonant acoustic excitation in a rocket combustion chamber with the combustion processes can result in the transfer of energy released due to the combustion process into the acoustic excitation. Under specific conditions this energy transfer can be very efficient resulting in combustion instabilities. These instabilities are still a key issue in the development of rocket combustors[1),2)]. If a combustion chamber can't be operated with sufficient stability margins the application of damping elements may guarantee stable operation. Helmholtz cavities are one option to dissipate acoustic energy[3),4)].

The experiments described in this paper address the interaction between acoustic waves and burning LOX/H_2- and LOX/CH_4-sprays. Periodic pressure fluctuations in the combustor are induced by releasing gas from the combustor by a secondary nozzle which is periodically blocked by a siren wheel. The setup allows realizing conditions where the reactive spray is exposed preferably to high acoustic pressure fluctuations or to high acoustic velocity fluctuations.

The secondary nozzle forms an additional cavity connected to the combustor. The experiments show that the resonance frequencies of the combustor are systematically changed due to the additional resonance volume. We give a short overview on the experimental phenomenology for combustors equipped with one absorber or an absorber ring.

For the propellant combination LOX/H_2 the combustion response has been analyzed for the situation with the reactive spray located either in a pressure node or in the pressure anti-node. The combustion response is analyzed based on dynamic pressure recordings and high-speed visualization of the flame emission. The spatially resolved flame emission and the pressure field reconstructed from the dynamic pressure sensors are used to discuss the coupling of acoustics to combustion.

2. Experimental setup

2.1 Combustion chamber

As tangential modes have been observed as the most critical excitations in rocket engines the combustor was designed to allow investigations at frequencies typical for these modes. A cross section of the combustion chamber is shown in Fig. 1. The chamber has a diameter is 20cm and a height of 4cm. The propellants are injected in radial direction with a coaxial injection element. The hot gases are released through the main nozzle, which is mounted in

the center of the face plate of the combustor. The other face plate can be equipped with a quartz window, giving full optical access to the combustor volume. With respect to the disk-like combustor volume and the radial injection of the propellants the set-up has been inspired by the experiments of Heidmann[5].

Due to the dimensions of the chamber the frequency of the first tangential mode is at about 4.0 kHz for LOX/H_2 and at 2.7 KHz for LOX/CH_4, thus the time scales of the interaction of the acoustic wave with the combustion chamber processes are representative for full scale rocket engines. Due to the small height of the combustor the longitudinal modes are at very high frequencies outside the range of the transversal resonances in this experiment.

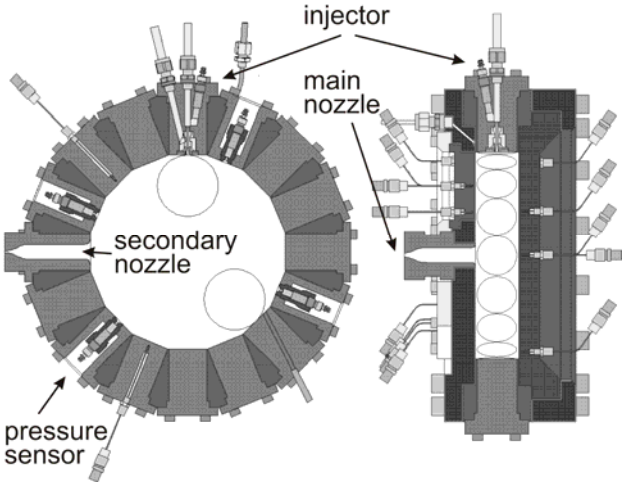

Fig. 1. Combustion chamber cross section

Propellants investigated are LOX/H_2 or LOX/CH_4. Hydrogen is injected at a temperature near to 100K, methane near to ambient temperature. The huge majority of tests up to now have been done with LOX/H_2, preliminary data on LOX/CH_4 are available.

2.2 Siren excitation

A secondary nozzle was be mounted in the cylindrical wall of the combustor with a throat diameter of 2mm. The throat area ratio of the main nozzle to the secondary nozzle varied between 6 and 25, depending on the main nozzle diameter.

By controlling the angular frequency of the siren wheel the excitation frequency could be adjusted. Usually the frequency was continuously increased during a test to excite subsequently several eigenmodes of the combustor.

The secondary nozzle could be mounted at different positions around the cylindrical wall of the combustor. An excited 1T mode has always a fixed orientation with respect to the secondary nozzle with its pressure nodal line perpendicular to the axis defined by the orientation of the secondary nozzle. The mounting the position of the secondary nozzle relative to the injection element is thus controlling the orientation of mode's nodal line relative to the spray axis. Two preferred situations have been examined. If the secondary nozzle is mounted at 180° relative to the injection element as shown in Fig. 2a the spray is exposed in the near injector region to maximum acoustic pressure fluctuations and the acoustic velocity is zero at the injector exit. Downstream the spray axis the value of the acoustic velocity is increasing with its direction parallel to the spray axis. When the nozzle is mounted at 90° relative to the injection element as shown in the sketch in Fig. 2b the pressure nodal line is in the spray region and the spray is exposed predominantly to acoustic velocity fluctuations. The velocity vector is perpendicular to the spray and the value of the acoustic velocity shows two maxima every period.

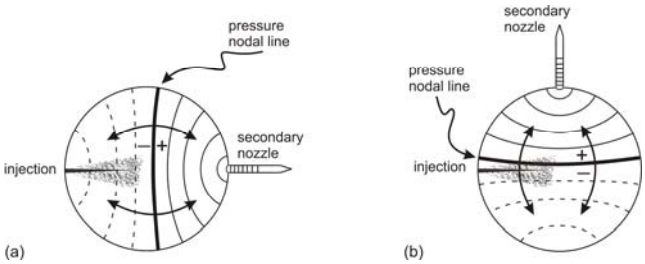

Fig. 2. Pressure fields in the combustor and nodal lines for 1T-excitation. (a) secondary nozzle at 180° and (b) secondary nozzle at 90° relative to injector.

2.3 Sensors and diagnostics

Up to 6 dynamic pressure sensors were distributed around the circumference of the combustor. The data acquisition rate of the dynamic sensors was 27 kHz.

High speed visualization was applied to record the dynamic response of the flame's chemiluminescence on acoustic excitation. The radiation of the OH-radical near to 307nm was recorded by an intensified CCD camera (Photron Ultima I2, 27000 frames/s, resolution 128x64 pixel).

3. Experimental Results

3.1. Acoustic resonances of the combustor

Resonance frequencies

During a test the excitation frequency was continuously increased. The time series of the measured dynamic pressure data during frequency ramping were analyzed by a sliding FFT. An example for the excitation of a LOX/H_2-flame is shown in Fig. 3. When ever the excitation frequency matches to an acoustic eigenmode of the combustor the power spectrum of the dynamic pressure exhibits a peak at the corresponding frequencies. The frequencies of the cylinder modes 2T and 1R are clearly visible in Fig. 3, however near the position, where the 1T resonance would be expected two resonance peaks are observed. It can be also seen that there are maxima in the acoustic power at the eigenfrequencies of the combustor due to the natural pressure fluctuations, independent of the excitation frequencies. A comparison of spectrograms for the combustor without secondary nozzle and with secondary nozzle resolves where to look for an explanation of the two resonances near the 1T frequency seen in Fig. 3. Without secondary nozzle the

resonances of the system correspond to the ones expected for a cylindrical resonance volume as can be seen in the left part of Fig. 4. When the secondary nozzle is mounted the 1T resonance is virtually split as shown in the right part of Fig. 4 whereas the other modes seem to be unaffected.

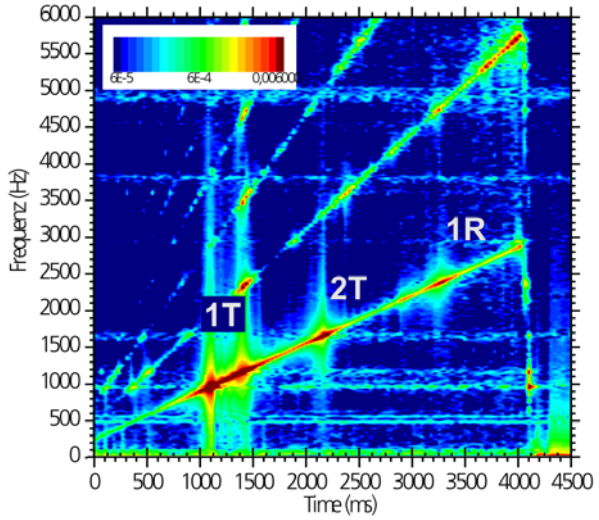

Fig. 3. Spectrogram of the combustion chamber pressure during ramping the excitation frequency in a LOX/hydrogen spray flame

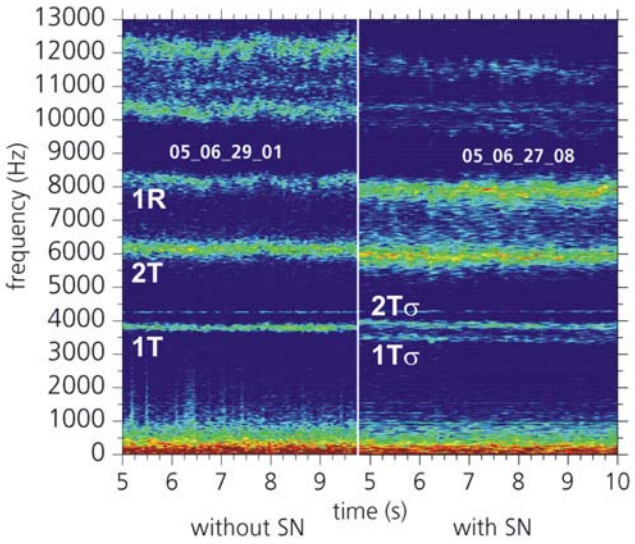

Fig. 4. Spectrogram of the combustion chamber pressure without external excitation. Left: without secondary nozzle, right: with secondary nozzle.

The mounting of the secondary nozzle is obviously changing the resonance characteristics of the system. G. Searby from the CNRS laboratory IRPHE first observed this phenomenon and highlighted the physical background. A sketch of the geometry of the secondary nozzle is shown in Fig. 5. The inlet of the nozzle forms a cylindrical volume that is acoustically coupled to the cylindrical combustor and the length of this inlet tube has been chosen by chance near to that of a quarter wave cavity. The similarity of the acoustic problem to that of an absorber cavity mounted to a combustor motivated to have a closer look to the situation[6]. The results of a numerical modal analysis and experimental measurements of the resonance frequencies for the coupled acoustic system comprising the combustor and an absorber cavity of variable length is shown in Fig. 6. It can be seen that with increasing cavity length the frequency of all eigenmodes are shifted to lower frequencies. Due to the rotational symmetry of the cylindrical combustor without absorber the tangential modes are twofold degenerate. With absorber the symmetry is broken and each degenerate tangential mode is split in two eigenmodes with components of different frequencies, labeled as σ- and π-component in the following. The σ-component is shifted to lower frequency, whereas the π-component is rather not influenced by the absorber. In Fig. 6 the length of the cavity formed by the inlet tube of the secondary nozzle is shown as a dashed line. Near to the 1T-resonance three resonances are predicted. A detailed analysis shows that only the 1Tσ and the 2Tσ resonance can be observed for the experimental situation realized in our experiment[6].

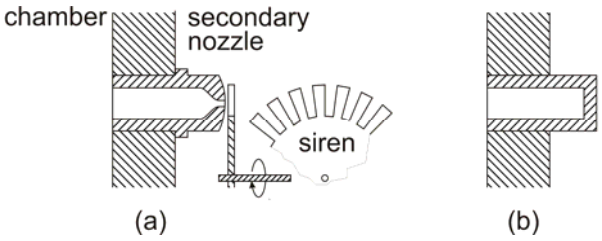

Fig. 5: (a) Sketch of the secondary nozzle and the siren wheel; (b) sketch of a quarter wave cavity.

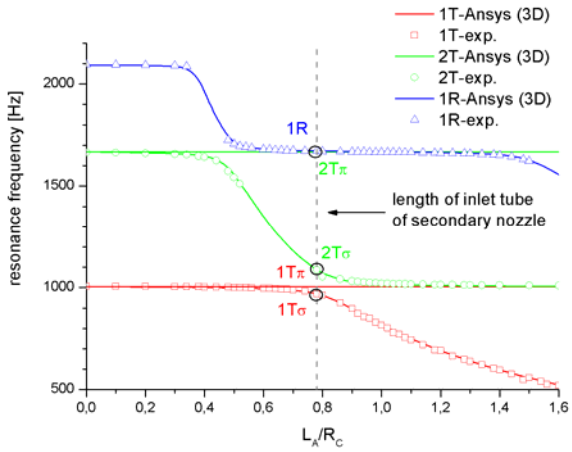

Fig. 6: Eigenfrequencies of a combustor with radius R_C equipped with an absorber tube of variable length L_A. The combustor was filled with ambient air.

Due to the relevance with respect to the mounting of quarter wave absorbers to combustors the investigation has been extended to an absorber ring. A 3D-mesh used for the analysis of the eigenmodes of a combustor equipped with an absorber ring is shown in Fig. 7 and the eigenfrequencies are shown in Fig. 8. As in the case for one absorber the eigenfrequencies of the combustor are

shifted to lower frequencies when an absorber ring is mounted. The resonance frequencies are grouping around the λ/4- and 3λ/4-resonances of the absorbers. The resonance spectra of a combustor with an absorber ring with $L_A/R_C = 0.82$ and without an absorber ring ($L_A/R_C = 0$) are presented in Fig. 9. Without absorber ring the resonances correspond to the cylinder modes. With absorber ring similar to the case with one absorber the 1T-resonance is virtually split. The value of $L_A/R_C = 0.82$ is shown in Fig. 9 as a dashed line and is near to an absorber tuned to a 1T-resonacne ($L_A/R_C = 0.8532$). A deeper analysis shows that the eigenmodes grouping near the absorbers λ/4-frequency are strongly damped and therefore cannot be seen in the resonance spectrum. Thus the experimental results nicely confirm the predictions from the modal analysis.

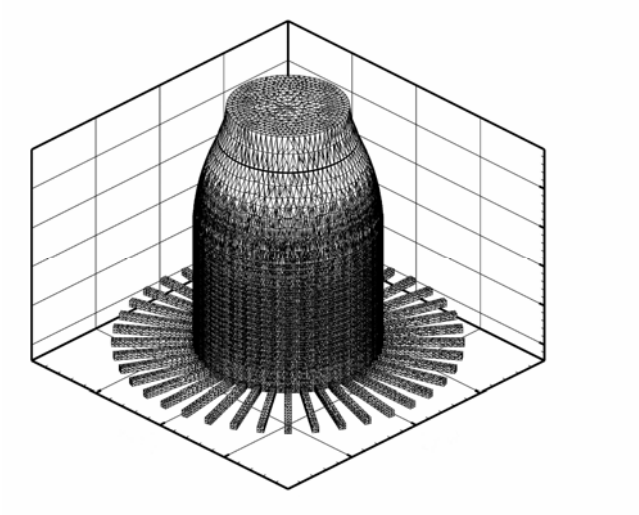

Fig. 7: 3D-mesh for numerical modal analysis of a combustor with an absorber ring.

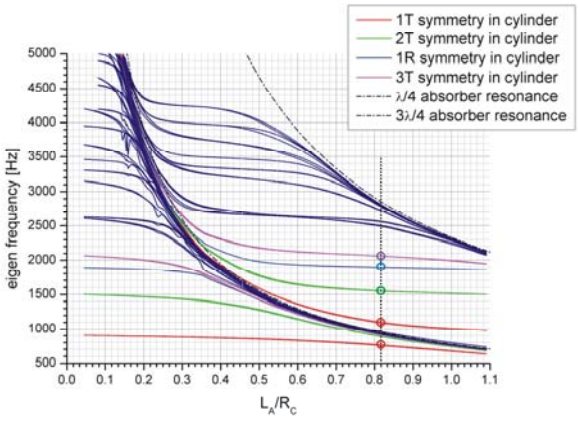

Fig. 8: Eigenfrequencies of a combustor with radius R_C equipped with an absorber ring with variable absorber length L_A.

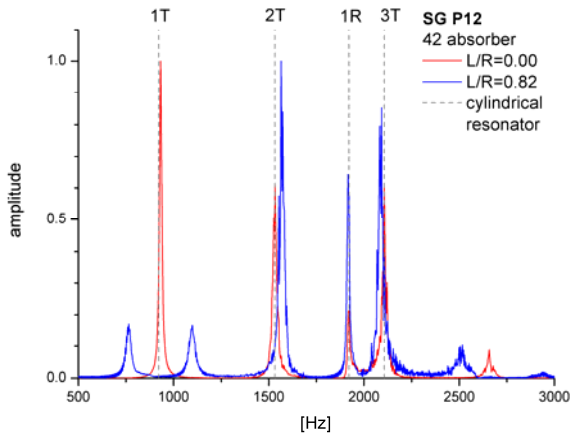

Fig. 9: Resonance frequencies of a combustor without (red) and with (blue) absorber ring.

3.2. Coupling of acoustics with spray combustion

Natural pressure fluctuations

The acoustic power of the natural pressure fluctuations in the 1T mode has been analyzed for various injection conditions for LOX/H_2. No correlation with fuel/oxidizer injection velocity ratio, momentum flux ratio or mixture ratio has been found. A significant dependence has been obtained between the Weber-number und the pressure response as shown in Fig. 11. The data show that there is a minimum value of We~5000 to see any power in the 1T mode, for higher We-numbers the pressure response is increasing with increasing We. It should be mentioned here that for the propellant combination ethanol/O_2 also a dependence on the We-number has been observed by Cheuret[7].

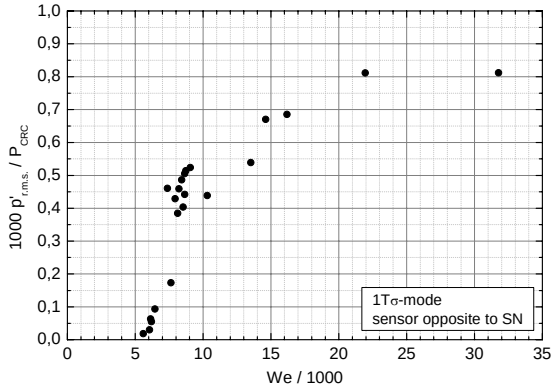

Fig. 11: Pressure response Δp/p as a function of the Weber-number for LOX/H_2.

Preliminary investigations with the combustor operated with LOX/CH_4 have just started. For comparison the spectrograms of the natural pressure fluctuations for both propellant combinations are shown in Fig. 10. Obviously the energy content of the pressure fluctuations in the individual eigenmodes is significantly different in both

cases. For example the 3T-mode is clearly visible for LOX/CH_4 and not for LOX/H_2, the 4T and 5T modes are visible in the spectrum of LOX/H_2, but not in the spectrum of LOX/CH_4. This may be an indication for differences in the interaction between the acoustics and combustion in both cases, but with the limited data available today for LOX/CH_4 it is too early to argue on the matter.

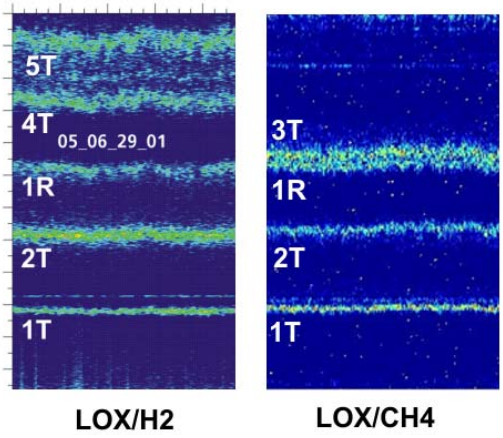

Fig. 10: Spectrograms of the natural fluctuations for LOX/H2 and LOX/CH4 combustion.

Combustion response during external excitation

With the quartz window the chemiluminescence from all the combustor volume could be recorded. The response of the combustion process to the acoustic field results in a modulation of the flame's OH-chemiluminescence $I(t)$. In Fig. 12 a local measurement of the temporal evolution of the OH-intensity is shown as measured with the high speed ICCD camera. The signal shows low frequencies variations due to the convective motion of flow volumes with different flame emission intensities. A small HF-signal at the excitation frequency with amplitude ΔI is superimposed.

The intensity of the chemiluminescence of the OH-radical $I(t)$ is regarded as an indicator for the heat release rate $\dot{q}(t)$. The amplitude $\Delta\dot{q}$ of the modulation of the heat release and its phase shift relative to the pressure fluctuation p' controls whether the coupling leads to an amplification of a damping of the acoustic excitation. This has been firstly discussed by Lord Rayleigh and the condition is expressed in his famous criterion[8)9)]

$$\int_V \int_t p' \cdot \dot{q}' \, dt dV > 0$$

Following Heidmann and Wieber[10)] a response factor N can be defined based on the Rayleigh criterion:

$$N = \frac{\int_V \int_t P' \cdot Q' \, dt dV}{\int_V \int_t P'^2 dt dV}$$

with $Q' = \dot{q}'/\dot{q}$ and $P' = p'/p$. With the assumption of harmonic time dependencies for $p' = \Delta p \cdot \cos(\omega t)$ and $\dot{q}' = \Delta\dot{q} \cdot \cos(\omega t + \varphi)$ this reduces to

$$N = \frac{\Delta\dot{q}/\dot{q}}{\Delta p/p} \cos(\varphi)$$

For an amplification of the acoustic wave the amplitude $\Delta\dot{q}$ has to be high enough to exceed losses and optimum amplification is obtained for a phase shift $\varphi = 0$. No phase shift between the fluctuating dynamic pressure and flame emission has been found in our experiments in the frame of the measurement accuracy indicating that the conditions for amplification would be fulfilled, if the gain due to combustion would exceed the losses.

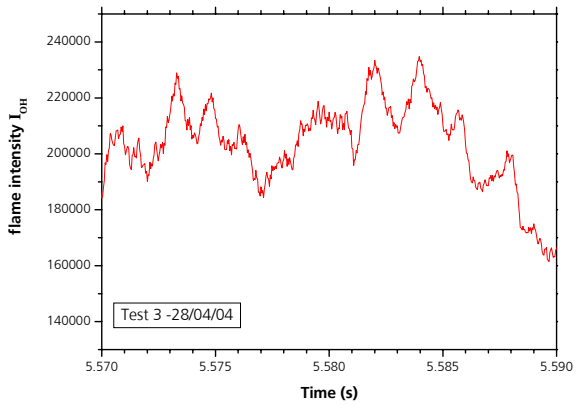

Fig. 12. Temporal evolution of the flame intensity during external excitation

For further analysis the measured intensity $I(t) = I + \Delta I \cdot \cos(\omega t + \varphi)$ of the chemiluminescence of the OH-radical is identified with the heat release $\dot{q}(t)$. As the OH emission was recorded with a high speed intensified CCD camera the spatial distribution of local mean value $I(x,y)$ and the amplitude $\Delta I(x,y)$ of the flame emission is available.

From the dynamic pressure sensors mounted around the circumference of the combustor the spatial distribution of the amplitude of the acoustic pressure field $\Delta p(x,y)/p$ is reconstructed. Thus the spatially resolved response factor $N(x,y)$ can be determined:

$$N(x,y) = \frac{\Delta I(x,y)/I(x,y)}{\Delta p(x,y)/p} \qquad (1)$$

The acoustic pressure and velocity fields for the excited 1T-modes have characteristic spatial distributions (see Fig. 2) depending on the mounting position of the secondary nozzle. The analysis of the flame emission response as a function of the orientation of the pressure nodal line is used to address the question whether the flame is coupled to the acoustic velocity or to the acoustic pressure.

Due to the limitation of the spatial resolution of the intensified high speed CCD-camera only the flame in the lower part of the combustor is visualized and the local flame response $\Delta I(x,y)/I(x,y)$ is determined in this region. From these data with the help of Eq. (1) the local response factor has been determined for the configuration with the siren at the 90°- and the 180°-position (see Fig.

2).

In Fig. 13a the mean value $I(x,y)$ and in Fig. 13b the amplitude $\Delta I(x,y)$ of the flame emission for excitation at the 90° position is shown. Both distributions shown high values on the spray axis whereas the amplitude of the flame emission ΔI exhibits another maximum below the spray axis (Fig. 13b). The relative flame response $\Delta I/I$ shown in Fig. 13c exhibits no more a maximum on the spray axis but a pronounced maximum in the lower half of the chamber. As can be seen in Fig. 2b for the 90°-excitation this is the location of the pressure anti-node. Thus the spatial distribution of $\Delta I/I$ reflects the symmetry of the pressure distribution of the excited 1T-mode. Note that for the excitation at 90° the acoustic velocity is maximum on the spray axis.

The results for the excitation at the 180° position are shown in Fig. 14a-d. The mean flame intensity is similar as in the 90° case, maximum intensity I is recorded on the spray axis (Fig. 14a). The amplitude of the flame intensity fluctuation ΔI shown in Fig. 14b exhibits two maxima at the locations of the pressure anti-nodes (see Fig. 2a). The flame response $\Delta I/I$ shown Fig. 14c is minimum in the region of the pressure nodal line.

The symmetry of the flame response $\Delta I/I$ thus reflects the symmetry of the pressure field for the case of the 90° and for the case of the 180° excitation. From these observation it is concluded that for the conditions of the experiment there is coupling of the LOX/H_2-spray flame to an acoustic wave and the coupling process is pressure sensitive.

The local response factor $N(x,y)$ should allow evaluating where for a given acoustic disturbance $\Delta p/p$ there is a heat release response represented by $\Delta I/I$. The response factor N is shown in Fig. 13d and 14d. For excitation at 90° $N(x,y)$ is maximum on the spray axis which is a very reasonable result, because sensitive processes (droplet vaporization, chemical reaction) are located in that region. For excitation at 180° a strong response is found on the pressure nodal line, which doesn't fit into the picture as there is only hot gas in the flow and no specific sensitivity to an acoustic excitation is expected. It has to mentioned that the calculated values of the response factor $N=(\Delta I/I)/(\Delta p/p)$ are very sensitive to the exact location of the assumed pressure nodal line where $\Delta p=0$. Furthermore the analysis showed that the results shown in Fig. 13a-c and 14a-c are reproducible, whereas the response factor derived from the data and shown in Fig. 13d and 14d exhibits significant statistical error. The accuracy of the measurements has do be improved for a quantitative evaluation of the response factor $N(x,y)$.

5. Summary and conclusions.

It has been shown that the mounting of a resonance volume to a cylindrical combustor has significant consequences for the values of the acoustic eigenfrequencies of the coupled acoustic system the eigenfrequencies are systematically shifted to lower frequencies. Furthermore additional resonances are observed at frequencies that are not in agreement with the predictions for a cylindrical combustor. It has been shown by numerical modal analysis and by experiments that this behavior is found also for a combustor with an absorber ring.

By recording the flame emission with a high speed camera and analyzing the acoustic field as determined by dynamic pressure sensors distributed around the circumference of the combustor the combustion response has been evaluated. Zero phase shift between the fluctuating OH-emission and the acoustic pressure has been found thus indicating that according to the Rayleigh criterion energy released in the combustion process can be transferred to the acoustic field.

From a comparison of the spatial symmetries of the excited acoustic fields and the fluctuating OH-emission it is concluded, that the observed flame response is due to pressure sensitive processes.

From the relative amplitudes of pressure and flame emission a response factor has been derived. Due to the limited quality of data available today a quantitative evaluation of the response factor could no be done.

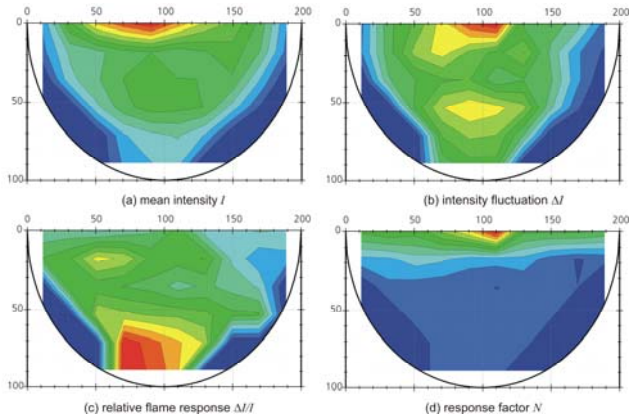

Fig. 13. Local mean flame intensity and flame response for excitation with the secondary nozzle and siren at 90°

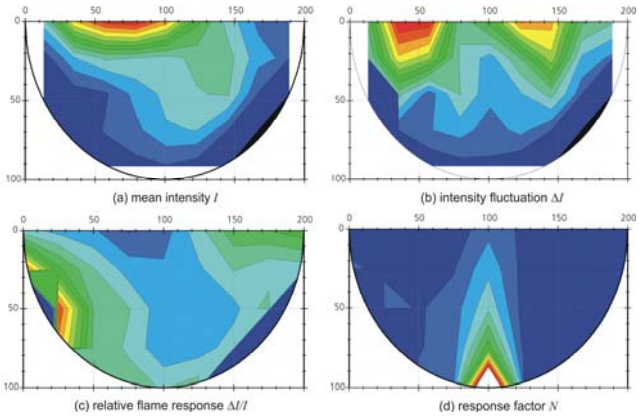

Fig. 14. Local mean flame intensity and flame response for excitation with the secondary nozzle and siren at 180°

References

1) Harrje, D.T., Reardon, F.H. (Eds.): Liquid Propellant Rocket Combustion Instability, *NASA, SP-194*, 1972
2) Yang, V., Anderson, W. (Eds.): Liquid Rocket Engine Combustion Instability, *AIAA Progress in Astronautics and Aeronautics*, Vol 169
3) Oberg, C.L., Wong, T.L., Ford, W.M.: Evaluation of Acoustic Cavities for Combustion Stabilization, *NASA CR 115087*, 1971
4) Laudien, E., Pongratz, R., Pierro, R., Preclik, D.: Experimental Procedures Aiding the Design of Acoustic Cavities, in *Liquid Rocket Engine Combustion Instability*, Yang, V. and Anderson, W. (Eds.), AIAA Progress in Astronautics and Aeronautics, Vol. 169, pp. 377-399, 1995
5) M.F. Heidmann, M.F.: Oscillatory Combustion of a Liquid-Oxygen Jet with Gaseous Hydrogen, *NASA TN-D-2753*, 1965
6) Oschwald, M., Farago, Z., Searby, G., Cheuret, F. : Resonance frequencies and damping of a cylindrical combustor acoustically coupled to an absorber, to be published in the *Journal of Propulsion and Power*, Vol. 24, 2008
7) Cheuret, F.: Instabilités thermo-acoustiques de combustion haute-fréquence dans les moteurs fuséees, PhD Thesis, Université de Provence, Marseille, Year = 2005
8) Lord Rayleigh, The Theory of Sound, Vol. II, p. 226, Dover, New York, 1945
9) Lord Rayleigh, The Explanation of Certain Acoustical Phenomena, *Royal Institution Proceedings*, pp. 536-542, Vol. VIII, 1878
10) Heidmann, M.F., Wieber, P.: Analysis of Frequency Response Characteristics of propellant Vaporization, *NASA TN-D-3749*, 1966